Edge Reconstruction and Emergent Neutral Modes in Integer and Fractional Quantum Hall Phases

Udit Khanna,[1] Moshe Goldstein,[2] and Yuval Gefen[3]

[1] *Department of Physics, Bar-Ilan University, Ramat-Gan 52900, Israel*
[2] *Raymond and Beverly Sackler School of Physics and Astronomy, Tel-Aviv University, Tel Aviv, 6997801, Israel*
[3] *Department of Condensed Matter Physics, Weizmann Institute of Science, Rehovot 76100, Israel*

This paper comprises a review of our recent works on fractional chiral modes that emerge due to edge reconstruction in integer and fractional quantum Hall (QH) phases. The new part added is an analysis of edge reconstruction of the $\nu = 2/5$ phase. QH states are topological phases of matter featuring chiral gapless modes at the edge. These edge modes may propagate downstream or upstream, and may support either charge or charge-neutral excitations. From topological considerations, particle-like QH states are expected to support only downstream charge modes. However the interplay between the electronic repulsion and the boundary confining potential may drive certain quantum phase transitions (called reconstructions) at the edge, which are associated to the nucleation of additional pairs of counter-propagating modes. Employing variational methods, here we study edge reconstruction in the prototypical particle-like phases at $\nu = 1, 1/3$ and $2/5$ as a function of the slope of the confining potential. Our analysis shows that subsequent renormalization of the edge modes, driven by disorder-induced tunnelling and intermode interactions, may lead to the emergence of upstream neutral modes. These predictions may be tested in suitably designed transport experiments. Our results are also consistent with previous observations of upstream neutral modes in these QH phases, and could explain the absence of anyonic interference in electronic Mach-Zehnder setups.

Mark Azbel was a physicist in his heart and soul. Beside his major contributions to the quantum theory of electrons in metals, he left his footprints everywhere through talks, arguments and discussions on a broad spectrum of issues (including non-physics themes). He would take an issue that appears all but benign, and expose the intricacy, deep significance, and a scale of insight needed to really penetrate the problem at hand. Among his many notable works was the prediction of the anomalous skin effect in metals [1, 2]. It is only natural to devote our manuscript in this commemorative volume to a study of another "skin" effect related to the boundary of a two-dimensional electron gas in the presence of a strong perpendicular magnetic field. This concerns the gapless chiral edge modes which emerge at the boundary of quantum Hall phases.

I. INTRODUCTION

Quantum Hall (QH) phases are two-dimensional topological phases featuring gapless, chiral modes localized at the boundary of the sample [3]. Since the bulk of a QH phase is gapped, its transport properties are controlled by the edge modes [4, 5]. The topological properties of the bulk QH phase guide the nature of these boundary modes [6]. For instance, conventional models suggest that integer and particle-like fractional phases support only *downstream* edge modes, while hole-conjugate phases may support modes with both (upstream and downstream) chiralities [7–10]. Disorder-induced tunneling and intermode interactions further renormalise such counter-propagating edge modes and, in certain situations, may lead to the emergence of upstream neutral modes [11–13]. Experimental signatures of these upstream neutrals have been observed in the $\nu = 2/3$ [14–17] and $\nu = 5/2$ phases [18], as well as in engineered geometries [19, 20].

However, recent transport experiments [21–23] suggest that, even for the 'simple' QH phases (such as the $\nu = 1$ or $1/3$), the edge structure is much more intricate and may not be described by orthodox models. Exciting the $\nu = 1$ edge at a quantum point contact (QPC), Ref. [21] observed an upstream flow of energy (but not charge). A similar experiment was performed for fractional QH phases in the lowest Landau level in Ref. [22]. They observed that partial transmission of charge current through a QPC is accompanied by upstream electric noise (with no net current) in several fractional QH phases (including Laughlin states). In a complementary study, Ref. [23] observed that the visibility of the interference pattern in an electronic Mach-Zehnder interferometer decreases as the filling factor (ν) is reduced from 2 to 1. Moreover, interference is fully suppressed for $\nu \leq 1$. These experiments suggest that the standard picture of particle-like phases, involving one or more downstream modes, is incomplete. Instead these results point to the presence of additional counter-propagating modes, some of which may be charge-neutral.

In the early 90s, it was realized that in the presence of a smooth confining potential at the boundary, electronic interactions may induce quantum phase transitions at the edge (which leave the bulk unperturbed). Such edge transitions (or edge reconstructions) may occur in both integer [24–33] and fractional [34–46] QH phases, as well as in time-reversal-invariant topological insulators [47, 48]. The reconstructed edge structure may differ in terms of the number, order, or even the nature of the edge modes.

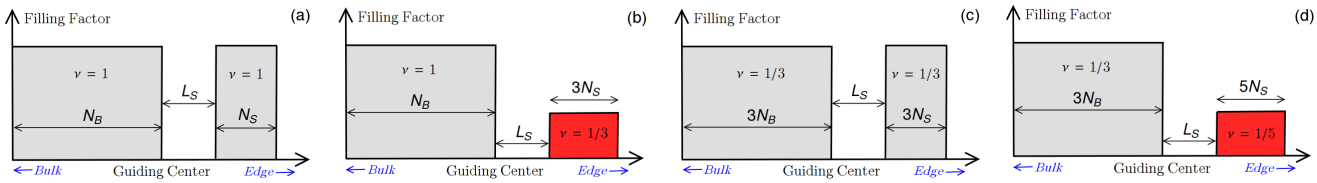

FIG. 1. A priori possible edge configurations for a bulk (a,b) $\nu = 1$ and (c,d) $\nu = 1/3$ phase. For a sharp confining potential, a single QH droplet (with $\nu = 1$ or $1/3$) composed of $N_B + N_S$ electrons is expected. As the edge potential becomes smoother, an additional side strip (separated from the bulk by L_S guiding centers) composed of N_S electrons is nucleated along the edge. The filling factor of the side strip may be the identical to [as shown in (a,c)] or different from [as shown in (b,d)] the bulk filling factor.

Such phase transitions are driven by the competition between the electrostatic effects of a smooth confining potential and the exchange/correlation energy of an incompressible QH state. For sufficiently smooth potentials, this competition leads to nucleation of additional electronic strips (in QH phases) along the edge [49, 50]. The nucleated side strips define additional pairs of counter-propagating chiral edge modes at their boundaries. Similarly to the edge of hole-conjugate states, intermode interactions and disorder-induced tunneling among these additional and the original (topological) edge modes may lead to a subsequent renormalization, modifying their nature qualitatively. Such renormalization may even give rise to additional (non-topological) upstream neutral modes [42].

Here, we describe our recent attempts [33, 45] to theoretically account for the experimental surprises described above, in terms of reconstruction and the subsequent renormalization of the edge for $\nu = 1$ and $1/3$ QH phases. Additionally, we present new analysis of edge reconstruction of the $\nu = 2/5$ QH phase. The main challenge here is to determine the precise filling factor of the additional side strip nucleated at the edge for a smooth confining potentials. An additional side strip of filling factor $\nu_{\rm strip}$ defines counter-propagating modes of charge $\nu_{\rm strip}$. Therefore, for $\nu_{\rm strip} = \nu_{\rm bulk}$ subsequent renormalization of the modes (due to disorder-induced tunneling) would lead to localization of a pair of counter-propagating modes and render transport experiments blind to the presence of reconstruction. On the other hand, for $\nu_{\rm strip} < \nu_{\rm bulk}$ subsequent renormalization would not induce localization, and may instead lead to the emergence of upstream neutral modes. Therefore, the experimental consequences of reconstruction crucially depend on the strip filling factor.

Figures 1, 2 depict some of the a priori possible configurations of the reconstructed edge at $\nu = 1, 1/3$ and $2/5$. Here, we find the lowest energy state among these structures as a function of the slope of the confining potential through a variational analysis [33, 34, 45], which allows us to include a large number of electrons while accounting for quantum correlations inherently present in QH states. Specifically, we treat the strip-size (N_S) and separation (L_S) as variational parameters. When the confining potential is sharp, we find the lowest energy state comprises a single QH droplet, i.e. no edge reconstruction. On the other hand, for sufficiently smooth potentials, we find that edge reconstruction leads to the emergence of a pair of additional counter-propagating gapless modes. Our results indicate that, in all three phases, the gapless modes of the reconstructed edge, and their subsequent renormalization leading to the emergence of neutral modes, may account for the experimental results reported in Refs. [21–23]. We also analyze additional experimental consequences of edge reconstruction, such as in two-terminal transport.

II. MODEL HAMILTONIAN AND VARIATIONAL ANALYSIS

Here, we provide details of the theoretical model used to study the QH edge. We also describe the variational analysis employed to find the lowest energy edge configuration as a function of the slope of the confining potential.

A. Basic Setup

We analyze the QH edge in the disk geometry, which is convenient due to the presence of a single boundary even for finite systems. We employ a rotationally symmetric gauge, $e\vec{A}/\hbar = (-y/2\ell^2, x/2\ell^2)$, where $\ell = \sqrt{\hbar/eB}$ is the magnetic length. The rotational invariance allows the single-particle states to be labelled by eigenvalues of the angular momentum ($\hat{L}$). We denote the states in the lowest Landau level (LLL) as ϕ_m with $m = 0, 1, 2, \ldots$. The corresponding wavefunction is $\phi_m(\vec{r}) = (r/\ell)^m e^{-im\theta_{\rm r}} e^{-\left(\frac{r}{2\ell}\right)^2} / \sqrt{2^{m+1}\pi m! \ell^2}$, where $re^{-i\theta_{\rm r}} = x - iy$ is the electronic position. The state ϕ_m is strongly localized around $r = \sqrt{2m}\ell$ and has angular momentum $\hbar m$.

In the LLL, the dynamics may be described by the Hamiltonian $H = H_{\rm ee} + H_{\rm c}$, where $H_{\rm ee}$ is the two-body electronic repulsion and $H_{\rm c}$ is the one-body confining potential (also assumed to be circularly symmetric). Note that H commutes with $\hat{L}$. Therefore, the many-body states may be labelled by the total angular momentum. Defining $E_c = e^2/\epsilon_0\ell$ as the Coulomb energy scale and $c_{m\sigma}$ as the annihilation operator corresponding to ϕ_m

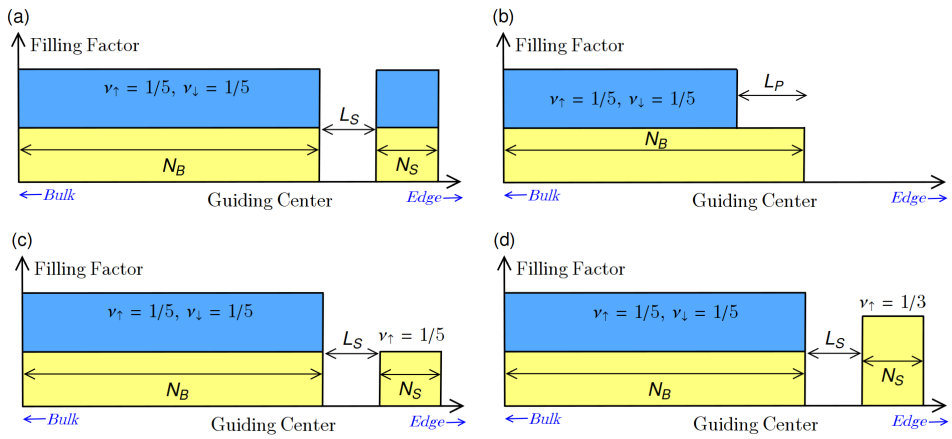

FIG. 2. A priori possible structures at the reconstructed edge for a (spin-singlet) $\nu = 2/5$ phase. The blue and yellow colors correspond to the two spin-polarizations of electrons in the lowest Landau level. Panel (a) depicts a spin-unpolarized edge configuration, while panels (b-d) depict structures with finite magnetization at the edge. Such spontaneous magnetization may arise without an additional stripe at the edge [as depicted in panel (b)] or due to the formation of such a stripe [panels (c,d)].

with spin state $\sigma = \uparrow/\downarrow$ (along s_z), we have,

$$H_{\rm ee} = \frac{E_{\rm c}}{2}\sum_{i\neq j}\frac{\ell}{|\vec{r}_i - \vec{r}_j|} \equiv \frac{E_{\rm c}}{2}\sum_{\{m,\sigma\},n} V^{ee}_{m_1 m_2;n} c^\dagger_{m_1+n\sigma_1} c^\dagger_{m_2\sigma_2} c_{m_2+n\sigma_2} c_{m_1\sigma_1}, \quad (1)$$

$$H_{\rm c} = \sum_{m,\sigma} V^{\rm c}_m\ c^\dagger_{m\sigma} c_{m\sigma}. \quad (2)$$

The confining potential is modelled using a positively charged background disk (with radius R, charge density $\rho_{\rm bg}$) separated from the electron gas by a distance d along the magnetic field [29, 36, 37]. The parameters R and $\rho_{\rm bg}$ are chosen such that overall charge neutrality is maintained. The electrostatic potential of this disk (in the plane of the electrons) is,

$$V_c(r) = \int_0^R dr' \int_0^{2\pi} d\theta \frac{E_c \rho_{\rm bg}}{\sqrt{d^2 + r^2 + r'^2 - 2r'r\cos\theta}}. \quad (3)$$

Then $V^{\rm c}_m$ in Eq. (2) are the matrix elements of $V_c(r)$. Note that the smoothness of this confining potential is controlled by the distance d (the tuning parameter in our analysis). Specifically, the edge potential is quite sharp for $d \sim 0$, and becomes smoother as d increases.

We note that edge reconstruction of both integer and fractional QH phases has been considered in previous works. These studies employed unbiased methods, such as exact diagonalization (ED) [29, 36, 37, 39, 40] and density matrix renormalization group (DMRG) [46, 51]. However, the precise filling factor at the edge cannot be obtained in ED due to its inherent limitation to small system sizes. By contrast, DMRG overcomes the size limitations of ED but works best for one-dimensional systems and its applicability to the problem of edge reconstruction is not clear. For these reasons, here we employ a variational method to study the edge [34]. Our method is capable of predicting the precise filling factor of the edge, and is not limited to a small system size. Moreover, such methods have been used extensively to study various aspects of QH phases [52] and their applicability is well established.

B. Variational Analysis

We consider several variational classes describing a priori possible edge structures for the $\nu = 1, 1/3$ and $2/5$ QH phases. All the classes considered here represent product states of a bulk QH droplet composed of N_B electrons, and a single edge strip composed of N_S electrons. The edge strip is separated from the bulk by L_S guiding centers. In our analysis, the total number of electrons $(N_B + N_S)$ is kept fixed. Therefore, the states in any of the classes may be parameterized by N_S and L_S. For a given bulk QH phase, each variational class corresponds to fixed filling factors for the bulk and the edge strip. Figures 1 and 2 depict the various classes of variational states considered in this work.

The $\nu = 1$ and $1/3$ phases are assumed to be fully spin-polarized (cf. Fig. 1). Therefore we consider spinless electrons in these cases. Then the bulk $\nu = 1$ phase represents a Slater determinant of N_B electrons, occupying all the guiding centers from $m = 0$ to $m = N_B - 1$. The bulk $\nu = 1/3$ phase is represented by the $\nu = 1/3$ Laughlin state. The Laughlin wavefunction corresponding to $\nu = 1/m_B$ is [52, 53],

$$\Psi_{\frac{1}{m_B},N_B} = \prod_{j>i}\left[\left(z_i - z_j\right)^{m_B}\right] e^{-\frac{1}{4}\sum_i |z_i|^2}. \quad (4)$$

Here $z_j = (x_j - iy_j)/\ell$ is the position of the jth electron. Next, the edge strip comprising the $\nu = 1$

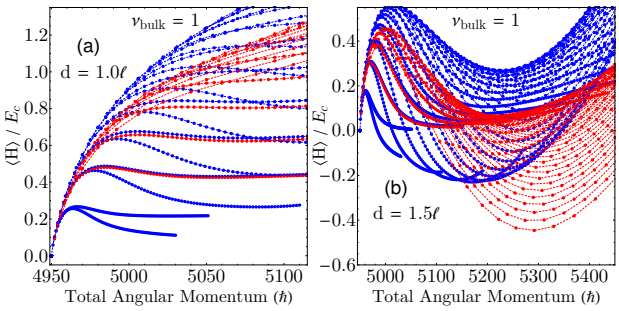

FIG. 3. Results of the variational analysis using 100 electrons with bulk filling factor $\nu = 1$. The blue (red) dots show the total energy of the variational states with a $\nu = 1$ integer ($\nu = \frac{1}{3}$ fractional) side-strip as a function of the total angular momentum for a (a) sharp ($d = \ell$) and (b) smooth ($d = 1.5\ell$) confining potential. Each curve corresponds to states with the same separation between the bulk and side-strip (L_S) but with different number of electrons in the side-strip (N_S). The curves shown here correspond to L_S varying from 0 to 30 guiding centers. The energy of the unreconstructed state has been subtracted to make comparison easier. (a) For sharp edges ($d < 1.3\ell$) the ground state is the one with minimum angular momentum, implying no edge reconstruction. (b) For smooth edges ($d > 1.3\ell$) the ground state shifts to a higher angular momentum sector, implying that the electronic disk expands and the edge undergoes reconstruction. The minimum energy state lies on the curve corresponding to $L_S = 0$. Panel (b) shows that a fractional reconstruction is energetically favorable to an integer reconstruction.

phase [Fig. 1(a)] may also be represented as a Slater determinant of N_S electrons. On the other hand, the edge strip comprising $\nu = 1/3, 1/5$ phases [Figs. 1(b-c)] are described through a $\nu = 1/m_S$ Laughlin state ($m_S = 3, 5$) with M_S quasiholes at the origin. The separation of the bulk and edge strip (L_S) is given by, $L_S = (M_S - 1) - \nu_{\rm bulk}(N_B - 1)$. The corresponding (unnormalized) wavefunction is,

$$\Psi_{\frac{1}{m_S},N_S,M_S} = \prod_{i=1}^{N_S}\left[z_i^{M_S}\prod_{j>i}\left(z_i - z_j\right)^{m_S}\right]e^{-\frac{1}{4}\sum_i |z_i|^2}. \tag{5}$$

In this work, we focus on the spin-unpolarized $\nu = 2/5$ phase, which may be described as the product state of two copies (one for each spin) of the $\nu = 1/5$ Laughlin phase, i.e. $\Psi_{\frac{2}{5},N_B} = \Psi_{\frac{1}{5},N_B/2,\uparrow} \otimes \Psi_{\frac{1}{5},N_B/2,\downarrow}$. The reconstructed edge in this phase could be 'simple' and identical to the bulk [as shown in Fig. 2(a)], or due to the additional spin degree of freedom, may be spontaneously spin-polarized [see Figs. 2(b-d)]. Interestingly, the latter possibility may occur even without the nucleation of an additional edge stripe [see Fig. 2(b)] (this is analogous to the edge structure described for the $\nu = 2$ phase in Ref. [25]). All these configurations may be described through product states of appropriate Laughlin states, as mentioned above.

For Slater determinants, the energy ($\langle H\rangle$) of the variational states may be evaluated trivially given the matrix elements of the Coulomb interaction and the confining potential [33]. On the other hand, for Laughlin states these may be evaluated using standard classical Monte-Carlo techniques [45, 52–55]. In our analysis, we evaluate the energy of the states in each variational class as a function of d, which controls the slope of the confining potential. The ground state for each QH phase, and the precise structure of the edge, is then found by comparing the energies of the states in the different classes. Note that the unreconstructed state (without an additional edge strip) is included in all classes (corresponding to $N_S = 0 = L_P$). It is the lowest energy state for sharp confining potentials ($d \sim 0$). By contrast, the ground state supports an additional edge strip (finite N_S, L_S or L_P) for smoother potentials. Finally, the structure of the edge in the ground state uniquely determines the number and nature of the low-energy chiral modes.

III. VARIATIONAL RESULTS

This section presents the results of our analysis of the edge structure for the $\nu = 1, 1/3$ and $2/5$ QH phases. In all cases, we find that edge reconstruction may lead to the emergence of side stripes with filling factor different from that of the bulk QH phase.

Figure 3 shows the total energies for the two classes of variational states corresponding to $\nu = 1$ as a function of the total angular momentum at different confining potentials (controlled by d). A total of 100 particles were used for these results. The blue dots correspond to integer edges [Fig. 1(a)] while the red dots correspond to the fractional edges [Fig. 1(b)]. For a sharp confining potential [$d < 1.2\ell$, Fig. 3(a)] the lowest energy state is the one with the minimal angular momentum (in this case $4950\hbar$). This corresponds to the unreconstructed $\nu = 1$ state with a single chiral edge mode. For smoother potentials [$d > 1.3\ell$, Fig. 3(b)], the lowest energy state has a much larger angular momentum ($5256\hbar$ for $d = 1.5\ell$ with $N_S = 18$ and $L_S = 0$) than the compact state. Note that the states with a fractional edge are found to have a lower energy than the states with an integer edge *whenever reconstruction is favored.* We have verified that our results do not depend on the detailed form of the confining potential [33]. The fractionally reconstructed edge [Fig. 1(b)] supports a downstream $e^* = 1$ mode (originating from the bulk) in addition to a counter-propagating pair of $e^* = 1/3$ modes arising from the side strip. Therefore, our results imply that *fractionally* charged chiral edge modes may exist even at the edge of bulk integer QH phases.

Figure 4 depicts the total energies of the states in the two classes corresponding to $\nu = 1/3$, classified by their angular momentum, for several values of d. These results correspond to a total of 50 particles. The blue (red) dots in Figs. 4(a-c) correspond to edges with a side strip

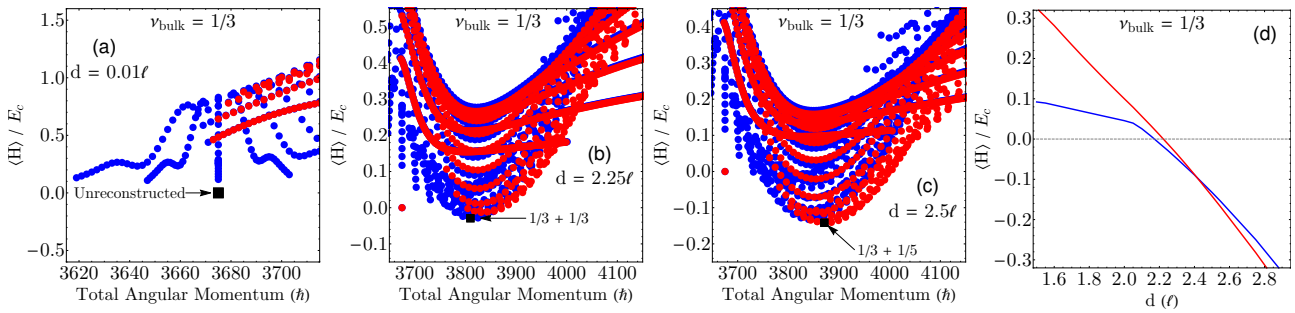

FIG. 4. Results of the variational calculations with 50 electrons with bulk filling factor $\nu = 1/3$. (a)-(c) The energy ($\langle H \rangle$) of the states in the two variational classes as a function of the total angular momentum at (a) sharp ($d = 0.01\ell$), (b) moderately smooth ($d = 2.25\ell$), and (c) very smooth ($d = 2.50\ell$) confining potentials. In all cases, the energy of the unreconstructed state ($\langle H \rangle_{\rm ur}$) has been subtracted. The blue (red) circles show energy of states with a side strip of $\nu = 1/3$ ($\nu = 1/5$). The black square marks the state with the lowest energy. (d) The variation of the lowest possible energy in the two variational classes with the smoothness of the confining potential (parameterized by d/ℓ). The blue (red) line corresponds to states with a side strip of $\nu = 1/3$ ($\nu = 1/5$). As expected, for sharp edges the ground state is the one with $N_S = 0$, corresponding to the unreconstructed $\nu = 1/3$ state with angular momentum $3675\hbar$. This state supports a single chiral $e/3$ mode. For moderately smooth potentials ($2.17 < d/\ell < 2.42$), an additional strip of $\nu = 1/3$ is generated at the edge, which gives rise to an extra pair of counter-propagating $e/3$ modes. For very smooth potentials ($d > 2.42\ell$) the additional strip has the filling factor 1/5. This second reconstructed state supports a counterpropagating pair of $e/5$ modes in addition to the chiral $e/3$ mode arising from the bulk.

of filling factor 1/3 (1/5). The black square marks the lowest energy state. In each case, we have subtracted the energy of the unreconstructed state ($N_S = 0$) to make the comparison easier. For a sharp confining potential [$d \lesssim 2.1\ell$, Fig. 4(a)] the standard Laughlin state, with no additional side strip, has the lowest energy (as expected). Such a state clearly has a single chiral $e/3$ mode at the edge. For smoother potentials [$d \gtrsim 2.1\ell$, Figs. 4(b-c)], the lowest energy state comprises an additional side strip ($N_S > 0$). This side strip may have filling factor 1/3 [Fig. 4(b)] for moderate slope of the confining potential ($N_S = 15$, $L_S = 11$ for $d = 2.25\ell$) or 1/5 [Fig. 4(c)] for very shallow slope of the potential ($N_S = 14$, $L_S = 3$ for $d = 2.5\ell$). Figure 4(d) shows the variation of the lowest possible energy in the two classes with the slope of the confining potential. Evidently, the filling factor of the side strip is 1/3 in the range $2.17\ell < d < 2.42\ell$, and switches to 1/5 for larger values of d. Hence, our analysis of the $\nu = 1/3$ edge suggests that upon reconstruction, it may support in addition to the single $e^* = 1/3$ mode arising from the bulk, a pair of counter-propagating $e^* = 1/3$ or (notably) 1/5 modes.

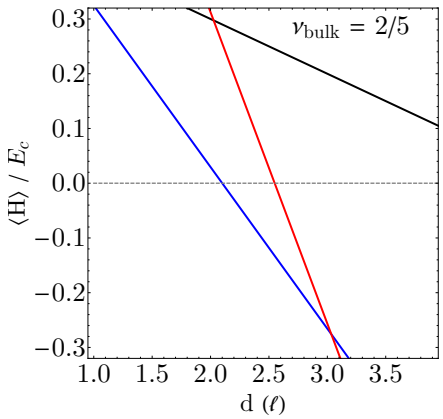

FIG. 5. Results of the variational calculations with 40 electrons with bulk filling factor $\nu = 2/5$. The curves show the variation of the lowest possible energy in the different variational classes as a function of the smoothness of the confining potential. The energy of unreconstructed state has been subtracted for ease of comparison. The black curve corresponds to spin-unpolarized edge, while the blue (red) curves correspond to spin-polarized edge structures without (with) an additional edge stripe. The red curve corresponds to an edge stripe in the $\nu = 1/3$ phase.

Figure 5 presents the lowest possible energy in the classes corresponding to $\nu = 2/5$ as a function of the slope of the confining potential. These are results for a total (including both spins) of 40 particles. The black line corresponds to the structure shown in Fig. 2(a) with a finite N_S (note that $N_S = 0$ corresponds to the unreconstructed state). Our analysis suggests that such a reconstruction is not energetically favorable for any slope of the confining potential. The blue line corresponds to reconstruction without an additional strip [Fig. 2(b)]. Clearly, this edge configuration is favorable (compared to the unreconstructed state) for $d > 2.0\ell$. The emergence of a spontaneous spin-polarization at the edge through a redistribution of the particles within the bulk (as opposed to the formation of a separate stripe) is analogous to the results of Ref. [25] for the bulk $\nu = 2$ state. Such a reconstruction does *not* lead to the emergence of new chiral modes. Rather, it only increases the spatial sep-

aration between the two bare (spin-polarized) $e^* = 1/5$ modes supported by the bulk state. However, our analysis suggests that for even smoother confining potentials ($d > 3.1\ell$), a separate edge stripe with $\nu = 1/3$ [Fig. 2(d)] is more favorable energetically (the red curve in Fig. 5 shows the lowest possible energy of this class). Such an edge structure has finite edge magnetization and supports an (additional) pair of counter-propagating $e^* = 1/3$ modes. Our results indicate that the structure shown in Fig. 2(c) is not energetically favorable in any range of d. For this reason, we do not show the energy of this class in Fig. 5. We thus conclude that for sufficiently smooth confining potentials, the spin-unpolarized $\nu = 2/5$ state may support at its edge, a pair of (spin-polarized) counter-propagating $e^* = 1/3$ modes in addition to the pair of downstream 1/5 modes of both spins.

IV. EXPERIMENTAL MANIFESTATIONS OF EDGE RECONSTRUCTION

The various configurations of the reconstructed edge found in our analysis may be uniquely identified in carefully designed transport experiments. Here, we focus on the behavior of the two-terminal conductance as a function of the sample length, and the manifestations of upstream neutral modes, which may emerge due to further renormalization of the edge modes.

A. Two-Terminal Conductance

Edge reconstruction is expected to have very clear consequences for the (electric) two terminal conductance ($g_{\text{2-ter}}$) as a function of the length of the edge (L). In a two-terminal setup, in the absence of edge equilibration, the chiral channels exiting the source contact are biased with respect to the modes entering it. The presence of impurities and potential disorder generates random tunneling between the chiral modes at the edge, which may facilitate intermode equilibration over a characteristic length ℓ_{eq} [56, 57]. Therefore, we may expect that $g_{\text{2-ter}}$ varies as a function of L over the equilibration length scale ℓ_{eq}. For $L \gg \ell_{\text{eq}}$, assuming full intermode equilibration, the two-terminal conductance is $g_{\text{2-ter}} = \nu_{\text{bulk}} \times e^2/h$ irrespective of the slope of the confining potential, reflecting the topological order of the bulk.

The $L \ll \ell_{\text{eq}}$ regime is more interesting, since the two terminal conductance is sensitive to the detailed structure of the edge in absence of intermode equilibration. For the unreconstructed edge (in the case of a sharp confining potential), $g_{\text{2-ter}} = \nu_{\text{bulk}} \times e^2/h$ for all values of L. This is because the unreconstructed edge supports only downstream mode (for the three phases considered here), rendering the notion of equilibration irrelevant.

For reconstructed edges the additional pair of counter-propagating modes may also contribute to $g_{\text{2-ter}}$. For

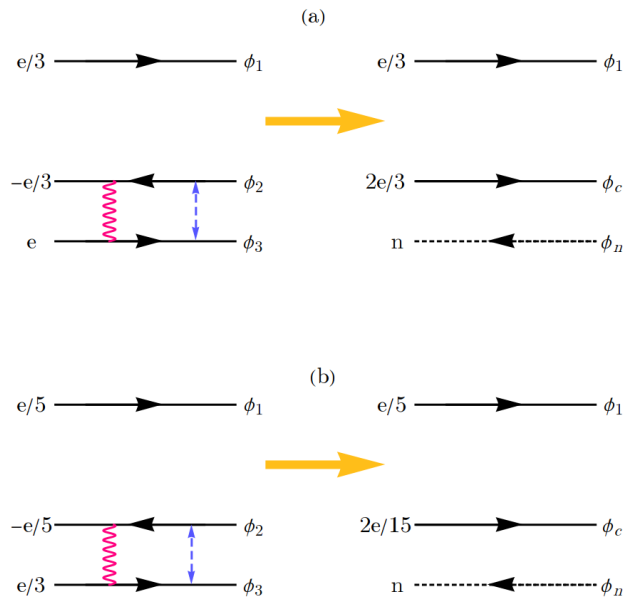

FIG. 6. For the edge structures in Figs. 1(b,d), the bare edge modes ($\phi_{1,2,3}$) are renormalized by intermode interactions (represented by the red wavy line) and disorder-induced electron tunneling (represented by the blue dashed line). Such renormalization may lead to emergence of a downstream charge (ϕ_c) and an upstream neutral mode (ϕ_n). In both cases, the outermost mode is assumed to be decoupled from the inner two modes, since our variational analysis indicates that, for smooth confining potentials, the distance between the outer mode and the two inner modes is much larger than the distance between the two inner modes.

the bulk $\nu = 1$ phase, the side stripe has filling factor $\nu = 1/3$. Then $g_{\text{2-ter}} = 5/3 \times e^2/h$ in very short samples. Note that the coefficient 5/3 uniquely determines the filling factor of the edge stripe. Hence, this is a *smoking gun* signature of our predicted edge structure. The reconstructed edge of the $\nu = 1/3$ phase, may support additional modes with $e^* = 1/3$ or 1/5 depending on the slope of the confining potential. Evidently, $g_{\text{2-ter}} = 1 \times e^2/h$ ($11/15 \times e^2/h$) in the former (latter) case. Finally, for the $\nu = 2/5$ phase, $g_{\text{2-ter}}$ is sensitive only to the 'second' reconstruction involving the formation of an additional $\nu = 1/3$ stripe. In this case, $g_{\text{2-ter}}$ increases to $16/15 \times e^2/h$. We note that the length dependence of the two-terminal conductance has been reported for other filling factors [58].

B. Emergent Non-Topological Neutral Modes

In the previous section, we relied on our variational analysis of the ground state in order to discern the nature of the chiral modes at the reconstructed edge. However, intermode interactions and disorder-induced tunnelling among these chirals may lead a subsequent renor-

malization of the bare edge modes. Such renormalization would lead to localization for identical (same e^*) counter-propagating modes. By contrast, counter-propagating modes of unequal charges (arising from QH regions of different filling factor) would be renormalized to two new effective modes of (in general, non-universal) charges $e^*_\uparrow$ and $e^*_\downarrow$ (here, $\uparrow/\downarrow$ denotes the direction of propagation: upstream/downstream) [11, 13]. Interestingly, in some cases $e^*_\uparrow$ may be zero leading to the emergence of gapless upstream neutral modes.

As explained previously, our variational analysis suggests that (for sufficiently smooth potentials) the filling factor of the additional side strip is not equal to the bulk filling factor, implying that chiral modes with differing e^* may be supported at the reconstructed edge. Our results also indicate that as the confining potential becomes shallower (d increases), the width of the edge stripe (N_S) increases much faster than its separation from the bulk (L_S). Hence, for very smooth confining potentials the outermost chiral mode couples very weakly to the inner pair of counter-propagating modes. Over sufficiently short length scales, we may assume that the outermost mode is completely decoupled from the other two. In this case, mode renormalization of the inner pair of counter-propagating chirals could lead to upstream neutral modes (ϕ_n in Fig. 6). Note that for simplicity, we only focus on the fully spin-polarized cases of $\nu = 1$ and $\nu = 1/3$ phases in this section.

The emergent neutral mode ϕ_n supports chiral flow of heat without an accompanying charge current, and hence has several unique manifestations in transport experiments. Such an upstream heat current was reported in Ref. [21] for the $\nu = 1$ phase. A biased neutral mode may also lead to generation of shot noise, despite the absence of a net charge current, due to the formation of quasiparticle-quasihole pairs [59–61]. Such observations were reported in Refs. [22, 23, 62] for various QH phases (including particle-like fractions). Additionally, the presence of upstream neutral modes may lead to the generation of shot noise on the (intermediate) conductance plateaus in the transmission of a quantum point contact. Interestingly, under certain situations, the Fano factor of this noise may be quantized and equal to the bulk filling factor ν_{bulk} instead of the quasiparticle charge [23, 63–65]. A complementary signature of upstream neutrals is the suppression of visibility of anyonic interference in electronic Mach-Zehnder setups [66]. This is in accordance with the observations of Ref. [23] for QH phases with $\nu \leq 1$.

V. CONCLUSIONS

We have employed variational analysis to study edge reconstruction that at the boundary of prototypical particle-like QH phases ($\nu = 1, 1/3$ and $2/5$). We have found that, in each case, edge reconstruction leads to the formation of an additional side strip, and that for sufficiently smooth potentials, the filling fraction of this side strip may be different from the bulk filling factor. Such a reconstruction has clear signatures in transport. We have pointed out some of these consequences related to the two-terminal conductance and the emergence of upstream neutral modes.

ACKNOWLEDGMENTS

We acknowledge illuminating discussions with Jinhong Park and Moty Heiblum. M.G. was supported by the Israel Science Foundation (ISF) and the Directorate for Defense Research and Development (DDR&D) grant No. 3427/21 and by the US-Israel Binational Science Foundation (BSF) Grants No. 2016224 and 2020072. Y.G. was supported by CRC 183 (project C01), the Minerva Foundation, DFG Grant No. RO 2247/11-1, MI 658/10-2, the German Israeli Foundation (Grant No. I-118-303.1-2018), the National Science Foundation through award DMR-2037654 and the US-Israel Binational Science Foundation (BSF), and the Helmholtz International Fellow Award. U.K. was supported by the Raymond and Beverly Sackler Faculty of Exact Sciences at Tel Aviv University and by the Raymond and Beverly Sackler Center for Computational Molecular and Material Science.

[1] M. Azbel and E. Kaner, Anamalous skin effect with arbitrary collision integral, Soviet Phys. JETP **2**, 749 (1956).
[2] M. Azbel, On the theory of skin effect in metals, Soviet Phys. JETP **5**, 1027 (1957).
[3] B. I. Halperin, Quantized Hall conductance, current-carrying edge states, and the existence of extended states in a two-dimensional disordered potential, Phys. Rev. B **25**, 2185 (1982).
[4] X. G. Wen, Electrodynamical properties of gapless edge excitations in the fractional quantum Hall states, Phys. Rev. Lett. **64**, 2206 (1990).
[5] X.-G. Wen, Theory of the edge states in fractional quantum Hall effects, International J. of Mod. Phys. B **6**, 1711 (1992).
[6] X. G. Wen, *Quantum Field Theory of Many-body Systems* (Oxford University Press, Oxford, 2007).
[7] X. G. Wen, Gapless boundary excitations in the quantum Hall states and in the chiral spin states, Phys. Rev. B **43**, 11025 (1991).
[8] X.-G. Wen, Edge transport properties of the fractional quantum Hall states and weak-impurity scattering of a one-dimensional charge-density wave, Phys. Rev. B **44**, 5708 (1991).

[9] A. H. MacDonald, Edge states in the fractional-quantum-Hall-effect regime, Phys. Rev. Lett. **64**, 220 (1990).

[10] M. D. Johnson and A. H. MacDonald, Composite edges in the ν=2/3 fractional quantum Hall effect, Phys. Rev. Lett. **67**, 2060 (1991).

[11] C. L. Kane, M. P. A. Fisher, and J. Polchinski, Randomness at the edge: Theory of quantum Hall transport at filling ν=2/3, Phys. Rev. Lett. **72**, 4129 (1994).

[12] C. L. Kane and M. P. A. Fisher, Impurity scattering and transport of fractional quantum Hall edge states, Phys. Rev. B **51**, 13449 (1995).

[13] I. Protopopov, Y. Gefen, and A. Mirlin, Transport in a disordered $\nu=\frac{2}{3}$ fractional quantum Hall junction, Annals of Physics **385**, 287 (2017).

[14] A. Bid, N. Ofek, M. Heiblum, V. Umansky, and D. Mahalu, Shot noise and charge at the 2/3 composite fractional quantum Hall state, Phys. Rev. Lett. **103**, 236802 (2009).

[15] A. Bid, N. Ofek, H. Inoue, M. Heiblum, C. L. Kane, V. Umansky, and D. Mahalu, Observation of neutral modes in the fractional quantum Hall regime, Nature **466**, 585 (2010).

[16] I. Gurman, R. Sabo, M. Heiblum, V. Umansky, and D. Mahalu, Extracting net current from an upstream neutral mode in the fractional quantum Hall regime, Nature Communications **3**, 1289 (2012).

[17] Y. Gross, M. Dolev, M. Heiblum, V. Umansky, and D. Mahalu, Upstream neutral modes in the fractional quantum Hall effect regime: Heat waves or coherent dipoles, Phys. Rev. Lett. **108**, 226801 (2012).

[18] B. Dutta, W. Yang, R. Melcer, H. K. Kundu, M. Heiblu, V. Umansky, Y. Oreg, A. Stern, and D. Mross, Novel method distinguishing between competing topological orders, arXiv:2101.01419 (2021).

[19] Y. Ronen, Y. Cohen, D. Banitt, M. Heiblum, and V. Umansky, Robust integer and fractional helical modes in the quantum Hall effect, Nature Physics **14**, 411 (2018).

[20] Y. Cohen, Y. Ronen, W. Yang, D. Banitt, J. Park, M. Heiblum, A. D. Mirlin, Y. Gefen, and V. Umansky, Synthesizing a ν=2/3 fractional quantum Hall effect edge state from counter-propagating ν=1 and ν=1/3 states, Nature Communications **10**, 1920 (2019).

[21] V. Venkatachalam, S. Hart, L. Pfeiffer, K. West, and A. Yacoby, Local thermometry of neutral modes on the quantum Hall edge, Nature Physics **8**, 676 (2012).

[22] H. Inoue, A. Grivnin, Y. Ronen, M. Heiblum, V. Umansky, and D. Mahalu, Proliferation of neutral modes in fractional quantum Hall states, Nature Commun. **5**, 4067 (2014).

[23] R. Bhattacharyya, M. Banerjee, M. Heiblum, D. Mahalu, and V. Umansky, Melting of interference in the fractional quantum Hall effect: Appearance of neutral modes, Phys. Rev. Lett. **122**, 246801 (2019).

[24] D. B. Chklovskii, B. I. Shklovskii, and L. I. Glazman, Electrostatics of edge channels, Phys. Rev. B **46**, 4026 (1992).

[25] J. Dempsey, B. Y. Gelfand, and B. I. Halperin, Electron-electron interactions and spontaneous spin polarization in quantum Hall edge states, Phys. Rev. Lett. **70**, 3639 (1993).

[26] C. d. C. Chamon and X. G. Wen, Sharp and smooth boundaries of quantum Hall liquids, Phys. Rev. B **49**, 8227 (1994).

[27] A. Karlhede, S. A. Kivelson, K. Lejnell, and S. L. Sondhi, Textured edges in quantum Hall systems, Phys. Rev. Lett. **77**, 2061 (1996).

[28] M. Franco and L. Brey, Phase diagram of a quantum Hall ferromagnet edge, spin-textured edges, and collective excitations, Phys. Rev. B **56**, 10383 (1997).

[29] Y. Zhang and K. Yang, Edge spin excitations and reconstructions of integer quantum Hall liquids, Phys. Rev. B **87**, 125140 (2013).

[30] U. Khanna, G. Murthy, S. Rao, and Y. Gefen, Spin mode switching at the edge of a quantum Hall system, Phys. Rev. Lett. **119**, 186804 (2017).

[31] A. Saha, S. J. De, S. Rao, Y. Gefen, and G. Murthy, Emergence of spin-active channels at a quantum Hall interface, Phys. Rev. B **103**, L081401 (2021).

[32] T. Maiti, P. Agarwal, S. Purkait, G. J. Sreejith, S. Das, G. Biasiol, L. Sorba, and B. Karmakar, Magnetic-field-dependent equilibration of fractional quantum Hall edge modes, Phys. Rev. Lett. **125**, 076802 (2020).

[33] U. Khanna, M. Goldstein, and Y. Gefen, Fractional edge reconstruction in integer quantum Hall phases, Phys. Rev. B **103**, L121302 (2021).

[34] Y. Meir, Composite edge states in the ν=2/3 fractional quantum Hall regime, Phys. Rev. Lett. **72**, 2624 (1994).

[35] A. H. MacDonald, E. Yang, and M. D. Johnson, Quantum dots in strong magnetic fields: Stability criteria for the maximum density droplet, Australian Journal of Physics **46**, 345 (1993).

[36] X. Wan, K. Yang, and E. H. Rezayi, Reconstruction of fractional quantum Hall edges, Phys. Rev. Lett. **88**, 056802 (2002).

[37] X. Wan, E. H. Rezayi, and K. Yang, Edge reconstruction in the fractional quantum Hall regime, Phys. Rev. B **68**, 125307 (2003).

[38] K. Yang, Field theoretical description of quantum Hall edge reconstruction, Phys. Rev. Lett. **91**, 036802 (2003).

[39] Z.-X. Hu, H. Chen, K. Yang, E. H. Rezayi, and X. Wan, Ground state and edge excitations of a quantum Hall liquid at filling factor 2/3, Phys. Rev. B **78**, 235315 (2008).

[40] Z.-X. Hu, E. H. Rezayi, X. Wan, and K. Yang, Edge-mode velocities and thermal coherence of quantum Hall interferometers, Phys. Rev. B **80**, 235330 (2009).

[41] Y. N. Joglekar, H. K. Nguyen, and G. Murthy, Edge reconstructions in fractional quantum Hall systems, Phys. Rev. B **68**, 035332 (2003).

[42] J. Wang, Y. Meir, and Y. Gefen, Edge reconstruction in the $\nu = \frac{2}{3}$ fractional quantum Hall state, Phys. Rev. Lett. **111**, 246803 (2013).

[43] Y. Zhang, Y.-H. Wu, J. A. Hutasoit, and J. K. Jain, Theoretical investigation of edge reconstruction in the $\nu=\frac{5}{2}$ and $\frac{7}{3}$ fractional quantum Hall states, Phys. Rev. B **90**, 165104 (2014).

[44] K. K. W. Ma, R. Wang, and K. Yang, Realization of supersymmetry and its spontaneous breaking in quantum Hall edges, Phys. Rev. Lett. **126**, 206801 (2021).

[45] U. Khanna, M. Goldstein, and Y. Gefen, Emergence of neutral modes in laughlin-like fractional quantum Hall phases, arXiv:2109.15293 (2021).

[46] L. Hu and W. Zhu, Abelian origin of $\nu = 2/3$ and $2+2/3$ fractional quantum Hall effect, arXiv:2109.00781 (2021).

[47] J. Wang, Y. Meir, and Y. Gefen, Spontaneous breakdown of topological protection in two dimensions, Phys. Rev. Lett. **118**, 046801 (2017).

[48] N. John, A. Del Maestro, and B. Rosenow, Robustness of helical edge states under edge reconstruction, arXiv:2105.14763 (2021).

[49] N. Paradiso, S. Heun, S. Roddaro, L. Sorba, F. Beltram, G. Biasiol, L. N. Pfeiffer, and K. W. West, Imaging fractional incompressible stripes in integer quantum Hall systems, Phys. Rev. Lett. **108**, 246801 (2012).

[50] N. Pascher, C. Rössler, T. Ihn, K. Ensslin, C. Reichl, and W. Wegscheider, Imaging the conductance of integer and fractional quantum Hall edge states, Phys. Rev. X **4**, 011014 (2014).

[51] T. Ito and N. Shibata, Density matrix renormalization group study of the ν=1/3 edge states in fractional quantum Hall systems, Phys. Rev. B **103**, 115107 (2021).

[52] J. K. Jain, *Composite Fermions* (Cambridge University Press, Cambridge, 2007).

[53] R. B. Laughlin, Anomalous quantum Hall effect: An incompressible quantum fluid with fractionally charged excitations, Phys. Rev. Lett. **50**, 1395 (1983).

[54] N. Metropolis, A. W. Rosenbluth, M. N. Rosenbluth, A. H. Teller, and E. Teller, Equation of state calculations by fast computing machines, The Journal of Chemical Physics **21**, 1087 (1953).

[55] S. Mitra and A. H. MacDonald, Angular-momentum-state occupation-number distribution function of the Laughlin droplet, Phys. Rev. B **48**, 2005 (1993).

[56] C. Nosiglia, J. Park, B. Rosenow, and Y. Gefen, Incoherent transport on the ν=2/3 quantum Hall edge, Phys. Rev. B **98**, 115408 (2018).

[57] C. Spånslätt, Y. Gefen, I. V. Gornyi, and D. G. Polyakov, Contacts, equilibration, and interactions in fractional quantum Hall edge transport, Phys. Rev. B **104**, 115416 (2021).

[58] F. Lafont, A. Rosenblatt, M. Heiblum, and V. Umansky, Counter-propagating charge transport in the quantum Hall effect regime, Science **363**, 54 (2019).

[59] J. Park, A. D. Mirlin, B. Rosenow, and Y. Gefen, Noise on complex quantum Hall edges: Chiral anomaly and heat diffusion, Phys. Rev. B **99**, 161302 (2019).

[60] C. Spånslätt, J. Park, Y. Gefen, and A. D. Mirlin, Topological classification of shot noise on fractional quantum Hall edges, Phys. Rev. Lett. **123**, 137701 (2019).

[61] C. Spånslätt, J. Park, Y. Gefen, and A. D. Mirlin, Conductance plateaus and shot noise in fractional quantum Hall point contacts, Phys. Rev. B **101**, 075308 (2020).

[62] R. Sabo, I. Gurman, A. Rosenblatt, F. Lafont, D. Banitt, J. Park, M. Heiblum, Y. Gefen, V. Umansky, and D. Mahalu, Edge reconstruction in fractional quantum Hall states, Nature Physics **13**, 491 (2017).

[63] Y. Cohen, Y. Ronen, W. Yang, D. Banitt, J. Park, M. Heiblum, A. D. Mirlin, Y. Gefen, and V. Umansky, Synthesizing a ν=2/3 fractional quantum Hall effect edge state from counter-propagating ν=1 and ν=1/3 states, Nature Comm. **10**, 1920 (2019).

[64] J. Park, B. Rosenow, and Y. Gefen, Symmetry-related transport on a fractional quantum Hall edge, Phys. Rev. Research **3**, 023083 (2021).

[65] S. Biswas, R. Bhattacharyya, H. K. Kundu, A. Das, M. Heiblum, V. Umansky, M. Goldstein, and Y. Gefen, Does shot noise always provide the quasiparticle charge?, arXiv:2111.05575 (2021).

[66] M. Goldstein and Y. Gefen, Suppression of interference in quantum Hall Mach-Zehnder geometry by upstream neutral modes, Phys. Rev. Lett. **117**, 276804 (2016).